

## MIT Open Access Articles

*Expansion microscopy: enabling single cell analysis in intact biological systems*

The MIT Faculty has made this article openly available. **Please share** how this access benefits you. Your story matters.

**Citation:** Alon, Shahar, Grace H. Huynh, and Edward S. Boyden, "Expansion microscopy: enabling single cell analysis in intact biological systems." FEBS journal 286, 8 (April 2019): p. 1482-94 doi 10.1111/febs.14597 2019 ©2019 Author(s)

**As Published:** 10.1111/febs.14597

**Publisher:** Wiley

**Persistent URL:** <https://hdl.handle.net/1721.1/124633>

**Version:** Author's final manuscript: final author's manuscript post peer review, without publisher's formatting or copy editing

**Terms of use:** Creative Commons Attribution-Noncommercial-Share Alike





Published in final edited form as:

FEBS J. 2019 April ; 286(8): 1482–1494. doi:10.1111/febs.14597.

## Expansion Microscopy: Enabling Single Cell Analysis In Intact Biological Systems

Shahar Alon<sup>1,2,7</sup>, Grace H Huynh<sup>1,2,3,7</sup>, and Edward S Boyden<sup>1,2,4,5,6</sup>

<sup>1</sup>Media Lab, Massachusetts Institute of Technology (MIT), Cambridge, USA

<sup>2</sup>McGovern Institute, MIT, Cambridge, USA

<sup>3</sup>Microsoft Research, Seattle, USA

<sup>4</sup>Department of Biological Engineering, MIT, Cambridge, USA

<sup>5</sup>Department of Brain and Cognitive Sciences, MIT, Cambridge, USA

<sup>6</sup>Koch Institute, MIT, Cambridge, USA

### Abstract

There is a need for single cell analysis methods that enable the identification and localization of different kinds of biomolecule throughout cells and throughout intact tissues, thereby allowing characterization and classification of individual cells and their relationships to each other within intact systems. Expansion microscopy (ExM) is a technology that physically magnifies tissues in an isotropic way, thereby achieving super-resolution microscopy on diffraction-limited microscopes, enabling rapid image acquisition and large field of view. As a result, ExM is well-positioned to integrate molecular content and cellular morphology, with the spatial precision sufficient to resolve individual biological building blocks, with the scale and accessibility required to deploy over extended 3-D objects like tissues and organs.

### Graphical Abstract

Expansion microscopy is a technology that physically magnifies tissues in an isotropic way, thereby achieving super-resolution with diffraction-limited microscopes. As a result, expansion microscopy is well-positioned to integrate molecular content and cellular morphology, and can be deployed over extended 3-D objects like tissues and organs. Figure adapted from Tillberg et al., Nat Biotechnol., 2016.

Correspondence: Edward S Boyden, Media Lab, McGovern Institute, and Koch Institute, Departments of Biological Engineering and Brain and Cognitive Sciences, MIT, Cambridge, MA 02139, USA, Tel: (617) 324-3085, esb@media.mit.edu.

<sup>7</sup>These authors contributed equally to this work.

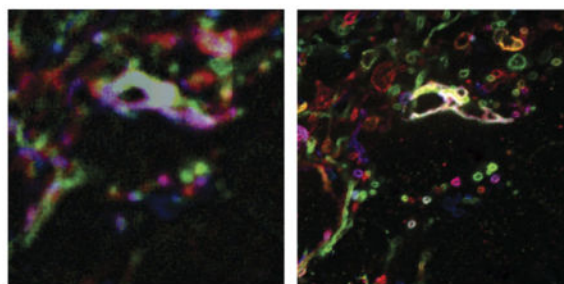
#### Competing financial interests

ESB is a co-inventor on multiple patents relating to ExM, and is also a co-founder of a company (<http://extbio.com/>) that aims to provide kits and services relating to ExM to the public. SA is a co-inventor on several patents relating to ExM.

#### Author contributions

All authors wrote the review. The order of co-first author names was determined by a coin toss.

### Expansion microscopy



Mouse hippocampus with Brainbow

### Keywords

Expansion microscopy; single cell analysis; morphology; genomics; FISH; multiplexing; super-resolution microscopy

## Can we measure the diversity of cells?

A long sought-after goal of biology is to unravel how cells are internally configured, and organized in tissues, in health and disease. The huge number of cells in mammalian tissues and their diverse properties makes this goal challenging. In recent years, thanks to the NIH Single Cell Analysis Initiative, the Chan Zuckerberg Initiative / Human Cell Atlas Consortium [1], the Cancer Research UK Grand Challenge, and the BRAIN Initiative Cell Census Network (BICCN), the question is increasingly posed: can we measure the diversity of cells, characterizing the key molecular determinants of healthy functions and disease states, in a comprehensive way? Given that even deciding what molecular mechanisms is most important is still an open scientific question, we propose that developing new tools that are easily extensible to the measurement of many kinds of cellular property – genomic, transcriptomic, proteomic, morphological – might be of great use in empowering individual scientists and groups to do single cell analysis appropriate to confront their specific scientific questions.

## Cell types and cell states

A common practice to explore cellular heterogeneity is to group cells into types, which are defined by a set of features that can each be quantitatively evaluated, making each cell a point in a high dimensional space, and a cell type a cloud of such cells [2]. A main driver of this way of thinking is that recent advances in genomics are allowing, for the first time, very high throughput and modest cost sequencing of DNA, of epigenetic signatures, and of expressed genes in RNA form, with single cell resolution. For example, one popular method is to microfluidically separate cells into nanoliter droplets, so that each cell's RNA content can be associated with a different nucleic acid barcode (i.e. a random sequence of nucleotides that serves as a unique cellular identifier); then, all the mRNAs can be sequenced via conventional means with the cell-specific barcodes allowing for assigning the

transcripts to be mapped onto individual cells [3]. These advances are considered essential for characterizing cell types and cell states (i.e., finer-scale variations in cells within a cell type), and their ease of use is already helping with the formulation of more precise definitions of cell type [4]. In particular, individual cells of the same type can no longer be viewed as identical units [5]. Instead, considerable variation in gene expression is observed even within a single cell type [4]. Concepts from the field of dynamical systems are used to describe these recent findings; as with other nonlinear systems, one or more possible solutions, termed attractors, are possible for any given cell. In this framework attractors represent cell types or stable cell states. Cells of a given type generally vary in their states, across populations of cells and over time, by presenting properties at different regions within one attractor, but cells can also move away from a given attractor, even changing cell fate entirely, and therefore large cell-cell variability is expected, in many biological and medical contexts [6]. As examples, cells can engage in a transformation that takes them on a trajectory between two attractors, as during the process of cell differentiation, or even sometimes stay stably in between two attractors, a topic which has not been as explored as other topics in the space of cell typing.

### **The need for multiplexed measurement of different kinds of biomolecules**

New technologies are clearly needed to make single cell analysis more powerful, accurate, and informative. Given that the relationship between the DNA, the RNA, and the proteins in a cell is subject to regulation at the transcriptional, translational, and post-translational steps, surprising insights might emerge if more than one type of molecule was commonly measured within the same cell, a practice that is not yet as common as the analysis of one molecular type. In practice this is challenging, since current experimental methods don't allow this high level of multiplexing; for example, most methods for single cell RNA sequencing require the destruction of the DNA and the proteins, and most methods for proteomic analysis require the destruction of the DNA and the RNA. The difficulty in performing simultaneous multimodal measurements is unfortunate, as the alternative, namely analyzing one parameter across one set of cells, and then measuring another parameter across another set of cells, can lead to false conclusions. The two sets of parameters, thus measured, are often jointly analyzed by averaging each parameter across the individual cells used to perform the measurement, with the assumption that a cell with all parameters equal to the means of their observed values would be typical [7]. However, the mean cell thus calculated may not be a typical, but rather may lie outside the population itself [7]. By measuring different parameters on different cells, perhaps even from different organisms, internal correlations that may indicate novel and important biological mechanisms will be missed. An inspiring example is the measurement of various ion channel mRNA counts in individual identified neurons of the crab stomatogastric ganglion [8]. When mRNA counts for a given potassium channel were analyzed for a given neuron type, across crabs, the mRNA counts appeared to vary wildly for those neurons, from crab to crab. But when two neurons of the same kind were analyzed within individual crabs, it became clear that the mRNA counts for that potassium channel were very similar within a given crab, even though the crab-to-crab variability was high. This observation predicts the existence of a novel molecular mechanism that enables two neurons of the same class to co-

regulate their gene expression, perhaps by the influence of a third party, or because of an emergent process occurring between the neurons.

## The importance of morphology for cell types and cell states

Of course, molecular content, extensive as it may be, is only one of the relevant properties in naming cell types and interpreting the biological functions of cell states [2]. Morphology -- both in regards to the configuration of molecules within cells in structured cascades (e.g., in neural and immunological synapses and other cell-cell contacts, highly scaffolded signal transduction pathways, nuclear chromatin structure, organelle-hosted metabolic pathway assemblies, and others) -- as well as in the context of how cells are organized into complex tissues and organs -- is completely lacking in most current high-throughput single-cell characterization methods, which require the dissociation of the tissue into single cells in suspension, and then the destruction of the cells themselves. Especially for the brain, where the details of cellular connectivity are essential for understanding the importance of a given cell type in neural information processing, the requirement for dissociation of tissues for RNA sequencing (for example) means that some information is currently permanently discarded in a typical single-cell analysis. Without knowing where a given brain cell type receives information from, or where a given brain cell type projects to, the role that a given cell type plays in neural computation can remain unclear. In addition, hypotheses about the origins of some diseases involve the initiation of pathology at sites within an organ which also would benefit from morphological investigation. Other kinds of biological questions, such as understanding the tumor microenvironment for a cancer cell, or examining how a developing organ self-assembles, face similar issues. As just one example, a morphology-informed single-cell characterization of the mouse liver revealed that cells expressed members of a given enzymatic cascade in a spatial pattern that mapped directly onto their temporal order of involvement in bile acid synthesis, suggesting a division of labor within the liver that would have been otherwise missed [9]. Throughout much of biology, microscopy and imaging have proven important for understanding how molecules play roles in emergent cellular functions. Bringing these strategies into the realm of characterizing cell types and cell states may greatly enhance the ability of scientists to define the most important aspects of cell types, regarding their function and dysfunction.

## Nanoscale localization of individual biological building blocks

Importantly, spatial information is important not only on the tissue level, i.e. the location of the cells inside the tissue, but also on the cellular level, i.e. the location of molecules within cells, and their relative organization with respect to each other. Recent interest in techniques such as cryo-EM has been driven in part by the desire to map how proteins work together in mesoscale structures to mediate complex functions. Super-resolution methods and electron microscopy have yielded a wide variety of insights into how proteins are organized with nanoscale precision. As just one example, a key component of neuronal communication is that each neuron can receive external signals from thousands of other neurons, connecting via synapses to different physical positions on the neuron surface. The signaling capacity of the synapses, and as a result the neuron's ability to respond to spatially different inputs, is realized by the nanoprecise subcellular distribution of molecules. A striking example is of

N-methyl-D-aspartate receptors (NMDARs), ion channel proteins that are gated by the neurotransmitter glutamate. Nanoscale differences in the location of NMDARs can determine the functional output of NMDAR signaling in downstream physiological processes. While stimulation of NMDARs located at synaptic clefts can promote neuronal survival, stimulation of NMDARs just 100 nm away can contribute to neuronal death [10]. This is because activation of synaptic versus extrasynaptic NMDARs have opposing effects on downstream signalling cascades [10]. Thus, nanoscale differences in the location of a protein can yield different, even opposite, changes in downstream cellular processes.

The nanoscale spatial organisation of receptors and signalling proteins is also crucial for mechanisms underlying immune cell activation [11]. A specific example is that of proteins which regulate T cell activation. T cells recognize exogenous (or endogenous) antigens on antigen-presenting cells (APC) with specificity determined by the T cell antigen receptor (TCR), which starts the T cell activation process after binding to the linker for activation of T cells (LAT). By using super-resolution imaging it was discovered that, rather than mixing freely in the plasma membrane, TCRs and LAT molecules are under strict spatiotemporal control [12]. According to one model, before APC binding, TCRs and LAT molecules form distinct and stable membrane domains (termed 'protein islands') with average radii of 35–70 nm, whereas APC binding brings these domains together [13]. Thus, nanoscale super-resolution imaging revealed a spatio-temporal regulation of the receptors and the signaling molecules in the plasma membrane, and possibly a previously unrecognized mechanism of T cell activation. Considering the molecules independently, without considering their organization relative to one another, would not yield an understanding of how they work together to make a single cell do what it does. Many other examples of this exist, particularly within signaling cascades, in a diversity of cell types, including sensory transduction molecules [14], G-protein coupled receptors [15], inhibitory synapse receptors [16], and protein kinases [17]. The highly scaffolded and spatially organized nature of many signaling cascades is thought to contribute to their modularity, speed, regulatability, specificity, and robustness [17]. The technology we propose, expansion microscopy (see below), increases tissue size. So expansion microscopy may be helpful for characterization of cell types because it enhances the ability to examine the organization of molecules within cells, but it may incur a cost, namely that fewer cells will be imaged in a given field of view. However, given that new kinds of high speed microscopes are currently being invented that can image increasingly large fields of view, such as light-sheet microscopes that can image expanded specimens extremely efficiently [49], this tradeoff may not be as severe as it initially looks. Diffraction limited microscopes such as light-sheet microscopes are increasing in speed and volume imageable faster than super-resolution microscopes are, which makes the pairing of light-sheet and expansion a particularly interesting one.

## The promise of in situ interrogation of intact tissues

In summary, in situ approaches utilizing imaging to assess the identity and location of specific biomolecules are well-positioned to allow molecular content to be profiled within the context of intact tissues and perhaps even intact organisms. Cell morphology can be preserved as well as the spatial location of molecules inside cells, and cells throughout tissues. Moreover, multiplexed in situ methods, such as multiplexed fluorescent in situ

hybridization (FISH) methods capable of imaging the location and identity of hundreds to thousands of transcripts in individual cells in tissues [18,19], and in situ sequencing methods capable of sequencing RNAs in individual cells in their intact states [20,21], are rapidly improving, so that many different biomolecules can be interrogated simultaneously. However, there are several challenges with current in situ approaches. Most of the challenges are a result of the fact that cells are densely packed with  $10^9$  DNA bases,  $10^8$  mRNA bases, and  $10^{12}$  amino acids, as well as lipids and carbohydrates, all jammed into a space typically a few microns in diameter [22]. Therefore, probing the molecules of interest is not trivial. This is especially true for thick tissues, where light scattering makes imaging inconvenient, and raises the requirement for deep-scanning methods such as two-photon microscopy, or for physical sectioning, which allows optical access and molecular labeling. Importantly, a growing number of tissue-clearing approaches have been instrumental in allowing in situ interrogation of thick tissue samples, including Scale [28], SeeDB [29], CUBIC [30], CLARITY [23], 3DISCO [24], iDISCO [25], PACT/PARS [26], SWITCH [27], and CUBIC-X [31]. Still, even if the molecules of interest are successfully targeted, reading out a dense signal is difficult with diffraction-limited microscopes, and capturing the nanoscale structural and organizational information is difficult. While super-resolution methods have been transformative in interrogation of specific samples, they are not easily scalable to large, sometimes thick, 3-D specimens typically analyzed in single cell analysis contexts, such as tissue specimens, brain circuits, and cancer biopsies. In summary, currently with in situ methods only a handful of markers are usually assessed at a given time, with typically only one molecule type (DNA, RNA or protein), and without nanoscale resolution [32].

## Expansion microscopy allow nanoscale precise single cell interrogation in intact tissues

Expansion microscopy (ExM) is a recently developed strategy for imaging molecular information throughout large cell and tissue samples, in 3-D and with nanoscale resolution, on ordinary diffraction-limited microscopes [33]. This is achieved by embedding the preserved sample (it does not preserve the living state, since it heavily chemically processes the tissue) in a matrix of swellable polymer, which is synthesized, from added monomers, throughout the specimen at a density on par with the density of biomolecules themselves, followed by homogenization (via heat, detergent, and/or enzymatic treatment) to enable molecules to be separated from each other, and finally isotropic physical expansion of the sample. While the concept of embedding samples in a polymer hydrogel matrix for improved imaging originated in the early 1980s by Hausen and Dreyer [34,35], such strategies have only recently been popularized through techniques such as CLARITY [23], which enables optical clearing of tissue and interrogation of thick tissue samples. In expansion microscopy, hydrogel embedding is performed with a highly swellable polyelectrolyte gel of crosslinked sodium polyacrylate, which swells when exposed to water. The phase transition physics of such swellable polymers was worked out by Tanaka and colleagues in the 1980s [36]. Synthesis of such polymers from their monomer building blocks, throughout cells and tissues, followed by expansion of the polymer-specimen



composite, has enabled nanoscale imaging of large intact cell and tissue samples [33,37,38], on ordinary high-speed diffraction-limited microscopes.

Specifically, this is done by first chemically tagging biomolecules and/or fluorescent labels so that they can be anchored to the polymer matrix (Fig. 1a). The polymer reagents (i.e. monomers, crosslinker, and activator) are diffused into the sample, and then the polymer is formed in situ. Varying the concentration of the polymer crosslinker controls the expansion factor of a given polyelectrolyte hydrogel, with higher levels of crosslinker resulting in less expansion, although the resultant distortion and resolution has not been systematically characterized except for the recipe that yields  $\sim 4.5\times$  linear expansion [33]. After polymerization, the tissue is then homogenized through heat treatment, detergent treatment, and/or enzymatic treatment, enabling isotropic expansion (Fig. 1b–c). The sample can then be expanded by placing it in water, at which point it becomes transparent, since it is mostly water (Fig. 1d). The process of expansion takes about a day, with actual hands-on-time of perhaps an hour or two for an experienced practitioner. After expansion, the tissue can be further processed for signal amplification or identification of biomolecules. Two rounds of expansion, aimed at enabling even greater physical magnification than achievable in a single round, can be achieved by using an iterative process. This is done by forming a second swellable polymer network within the space opened up by a first round of expanding a specimen; then, the original polymer network from the first round of expansion is degraded, and the newly synthesized network is expanded, for a second round of physical magnification [38].

The expansion process was designed to be highly isotropic and to provide high resolution in expanded samples. The density of reagents is set such that the spacing between polymer chains is estimated to be a few nanometers - around the size of a typical biomolecule [33,37–39]. In addition, the tissue homogenization step has been parameterized to minimize barriers to polymer expansion.

The isotropy and resolution of expanded samples has been estimated in a diversity of cell and tissue types. The gross expansion factor and isotropy can be measured by comparing features pre- and post-expansion and calculating the deformation via a non-rigid registration process. This enables quantification of the error of feature measurements. After a single round of  $\sim 4.5\times$  linear expansion, Chen et al. measured 1–4% distortion errors in measurements over length scales of tens to hundreds of microns (Fig. 1e–g; [33]), an error range that has now been replicated for multiple expansion protocols applied to a diversity of other cells and tissues, including human tissues [38,40–43]. Notably, this error varies non-linearly with the actual measurement length; larger lengths have less relative error (Fig. 1g). Alternatively, the resolution has been estimated by measuring the size of stereotyped structures such as microtubules [33], clathrin coated pits [33], and mitochondria [40] for which “ground truth” measurements are known from classical imaging methods such as electron microscopy, or for which comparisons could easily be made between pre- and post-expansion images. These measurements have resulted in estimates of the resolution of expansion microscopy to be  $\sim 60\text{--}70\text{ nm}$  for  $\sim 4.5\times$  expansion [40], very close to what might be expected for a  $\sim 300\text{ nm}$  diffraction limited lens if boosted in performance by  $\sim 4.5\times$  ( $\sim 300\text{ nm} / 4.5 \sim 60\text{--}70\text{ nm}$ ). After two rounds of expansion ( $\sim 4.5 \times 4.5 \sim 20\times$  expansion factor), a



resolution of ~25 nm was observed [38], slightly larger than the theoretical limit of ~300 nm / 20 ~ 15 nm. In this case, the resolution floor was likely limited by the size of the antibodies (~10–15 nm for the combination of primary and secondary antibody) used to crosslink the proteins of interest to the polymer network. Thus, even though the spacing between polymer chains is very small, as described above, applying antibody stains before expansion will limit the ultimate resolution to the size of an antibody.

Beyond these stereotyped structures, it remains an area of future research to determine if all sub-cellular regions expand isotropically down to very fine resolutions in the range of a few nanometers to tens of nanometers. For example, if there are regions of a cell which exclude or reduce the concentration of the reagents needed for polymerization, it is possible that these regions would be distorted and/or have reduced resolution compared to other tissue regions, at least for the existing expansion microscopy chemistries (although further chemical innovation may be able to alleviate these concerns). The nucleus, for example, is densely packed with DNA and other biomolecules, raising the question of what happens to the topology of the genome, at very fine length scales of nanometers to tens of nanometers, when the nucleus is expanded. Further, certain types of biomolecules may be less amenable to visualization using current versions of expansion microscopy. For example, biomolecules which are not well-fixed using standard formaldehyde-based fixation, like lipids, small molecules, and ions, are unlikely to be available for crosslinking into the polymer matrix, and hence would be difficult to visualize using expansion microscopy. However, new kinds of fixatives or preservation processes may be able to overcome this limitation of current expansion microscopy protocols. Finally, tissues that have been fixed with extremely strong fixatives may be difficult to expand isotropically, since such fixatives may impede even expansion. Future improvements in the fixation and expansion chemistries may alleviate such concerns.

## Nanoscale detection of proteins with expansion microscopy

Since the first report of expansion microscopy, many forms of the technique have been developed to enable nanoscale detection and localization of proteins via fluorescent antibody labeling or fluorescent protein fusion [33,37,38,40,42]. These methods directly anchor proteins to the swellable polymer matrix via a small molecule linker which reacts with free amines of proteins and can be copolymerized into the swellable, acrylate-based polymer matrix. Samples containing fluorescent proteins and/or fluorescent antibodies before polymerization can be expanded, enabling direct visualization of the fluorescent proteins and applied fluorescent antibodies (Fig. 2). Alternatively, samples can be expanded first and then antibody-stained post-expansion, taking advantage of the decrowding of epitopes that occurs when labels are applied post-expansion. This is an interesting case because it may be possible to label proteins in dense complexes, or with hidden epitopes, in a fashion that is not possible through any other microscopy technology. It may also be possible to achieve an additional resolution boost because the separation between proteins will be large, and thus the resolution loss due to non-zero antibody size would be reduced. One practical consequence of epitope decrowding is that diffusion of antibodies into samples is facilitated, and multiple rounds of labeling and destaining are enabled by the decrowding process

[33,37,38,40]. Indeed, such a method can be utilized with large scale tissue samples as large as an intact mouse brain.

The usability of ExM in probing subcellular location of proteins within complex natural environments has been demonstrated by many research groups working on a diversity of topics. In the short time since these technologies were published, already dozens of papers have begun to appear utilizing expansion microscopy to probe the relative organizations of proteins and other biomolecules. As just a few examples: Deshpande et al. [44] employed ExM to probe the subcellular organization of the astrocytic gap junction protein Cx43, in human brain specimens, revealing fine details of the organization of this protein amidst blood vessels and other cell types, and how this organization changed in the context of epilepsy. Crittenden et al. [45] used expansion microscopy to resolve the arrangement of striosomal fibers and dopamine-containing dendrites in the substantia nigra, revealing the densely intertwined nature of striosomal axons and dopamine-containing dendrites. Chozinski et al. [42] examined kinetochore structures in cells undergoing mitosis, revealing the detailed organization of cytoskeletal and associated proteins operating during cell division. The ability of ExM to allow for the examination of detailed cellular phenotypes in intact contexts is enabling it to make nanoscale and multiplexed molecular imaging into a simple element of the single cell analysis toolbox.

Expansion microscopy is compatible with a wide diversity of labeling strategies, microscopy platforms, and biological contexts. For example, the synaptonemal complex is a protein structure that forms between homologous chromosomes during meiosis, and is thought to help mediate chromosome pairing, synapsis, and segregation. Several studies have explored the 2D organization of components within the synaptonemal complex, and shown that the width of the structure, spanning between sister chromatids, ranges between 90–150 nm [46]. However, the density of the various structural components across this distance make it challenging to further characterize the 3D organization of the synaptonemal complex. Cahoon et al. [47] recently used expansion microscopy, followed by structured illumination microscopy, to directly visualize the transverse filaments spanning between sister chromatids. They were able to map out how different proteins dimerize and interact with one another, in this protein complex, by labeling different proteins in different locations and then performing expansion microscopy. Further work in this area could help elucidate the structural basis for accurate chromosome segregation during meiosis.

## Nanoscale detection of RNA with expansion microscopy

In addition to visualizing proteins, expansion microscopy has been adapted and used for visualization of DNA and RNA [41,48,49]. In expansion fluorescent in situ hybridization (ExFISH), RNAs are covalently anchored to the polymer matrix via a small molecule label that binds to guanine and can be copolymerized into the swellable, acrylate-based polymer matrix. After expansion, these RNAs are labeled with FISH probes [49] (Fig 3a–b). For low copy number mRNAs (Fig. 3c, lower left), the post-expansion transcripts are comparable in number to the pre-expansion transcripts, indicating high RNA integrity of the expansion process. For highly expressed mRNA transcripts however (yellow spots in Fig. 3c), more transcripts were detected after expansion than before expansion, indicating that the

expansion process decrowds transcripts that were previously indistinguishable, making them more precisely countable. Recently, Xiaowei Zhuang's group found that by combining their multiplexed fluorescence in situ hybridization method MERFISH with expansion microscopy, a 10-fold increase in the density of high-abundance RNAs could be obtained [50]. Labeling of RNAs can be easily multiplexed with ExFISH (Fig. 3d) and combined with protein labeling (Fig. 3e–f) using the techniques described above, to obtain information about both proteins and RNA in the same set of cells or tissues. One simply applies both the linker that binds proteins and the linker that binds RNA to the same specimen, so that both proteins and RNAs can be anchored to the polymer during the polymerization step.

Use of ExFISH can enable new insights into the localization and identity of specific mRNAs within cellular compartments. For example, the spatial organization of mRNA within neurons is important for neural development, and plays important roles in synaptic plasticity, learning, and memory [51]. The total number of dendritic mRNAs is notably smaller than the number of synapses, and consequently, some synapses lack the mRNA needed for immediate translation dependent plasticity [52]. Several studies have utilized in situ hybridization to estimate the sparsity of mRNAs within dendritic trees, but it remains challenging due to the spatial complexity of the dendritic tree and the wide variation in mRNA abundance, which can range over 3 orders of magnitude. By using ExFISH, Chen et al. [49] demonstrated 3D nanoscale imaging of the *Dlg4* mRNA, which encodes for the post-synaptic scaffolding protein PSD-95, and is known to be dendritically enriched (Fig. 3e–f). *Dlg4* mRNA was directly visualized within dendritic spines, which were filled with cytoplasmic YFP, which could be simultaneously imaged by using protein anchors in conjunction with RNA anchors. Consistent with the literature, individual *Dlg4* mRNAs were detected within a sparse subset of spines, and it was feasible to directly visualize the mRNAs within specific dendrites in the dendritic tree in situ within a thick 3D brain slice (Fig. 3e–f; [49]). Coupled with multiplexed coding schemes mentioned above, ExFISH holds promise for in situ characterization of RNA and synaptic organization in intact brain circuits.

## Clinical application of expansion microscopy

Expansion microscopy is spreading rapidly in biological and medical fields where single cell analysis is highly relevant. There are a wide range of samples that have been successfully expanded and imaged using expansion microscopy, including (in studies not described above) bacteria [53], the pathogen *Giardia* [54], the planaria *Schmidtea mediterranea* [55], isolated mitochondria [56], many kinds of cultured cells [48,57,58], diverse mouse tissues [59–62], a whole mouse brain [31], *Drosophila* [47], zebrafish [43], and diverse human tissues (Fig. 4; [41]). In many of these cases, expansion microscopy has enabled single cell analysis within intact tissues. Of translational interest, applying expansion microscopy may also help improve single cell characterization for a diversity of clinical applications. For example, the pathology classification of nuclear atypia in early breast lesions has proven to be challenging, partly because the information in traditional hematoxylin and eosin (H&E) stained images is limited by the optical diffraction limit. In contrast, by using a nuclear DAPI stain and expansion microscopy, computational detection and segmentation of nuclei was found to be significantly more accurate than in the H&E stained unexpanded case, and this improvement was borne out as an improvement of the diagnoses possible with machine

learning classification models trained on expert assessments [41]. This type of analysis could be used to support improved computational pathology analyses in the future.

## Summary

To better understand biological systems and improve clinical medicine, we will need multiplexed methods that integrate genomic data, molecular content, and cellular morphology, ideally with the spatial precision sufficient to resolve individual biological building blocks, and with the scale and accessibility required to deploy over extended 3-D objects like tissues and organs. Tools like expansion microscopy can help us to characterize and classify individual cells and their relationships to each other within intact systems. Expansion microscopy is easy to learn, with many protocols and tutorials available [63,64]. We are optimistic that integration of these data can help reveal new insights into fundamental questions of biology in health and disease.

## Acknowledgments

For funding ESB acknowledges the HHMI-Simons Fellowship, John Doerr, the Open Philanthropy project, IARPA D16PC00008, NIH Grants 1R01MH103910, 1RM1HG008525, 1R01MH110932, 1R01EB024261 and 1R01NS102727, the Cancer Research UK Grand Challenge, and U.S. Army Research Laboratory and the U.S. Army Research Office under contract/Grant Number W911NF1510548. SA is a HHMI fellow of the LSRF. We thank all members of the Synthetic Neurobiology group for helpful discussions.

## Abbreviations

<b>ExM</b>	Expansion microscopy
<b>BICCN</b>	BRAIN Initiative Cell Census Network
<b>NMDAR</b>	N-methyl-D-aspartate receptor
<b>CREB</b>	cyclic-AMP response element binding protein
<b>FOXO</b>	forkhead box protein O
<b>APC</b>	antigen-presenting cells
<b>TCR</b>	T cell antigen receptor
<b>LAT</b>	linker for activation of T cells
<b>FISH</b>	fluorescent in situ hybridization
<b>ExFISH</b>	expansion fluorescent in situ hybridization
<b>YFP</b>	yellow fluorescent protein
<b>H&amp;E</b>	hematoxylin and eosin
<b>DAPI</b>	4',6-diamidino-2-phenylindole
<b>RMS</b>	root mean square
<b>iExM</b>	iterative expansion microscopy

**smFISH**

single molecule fluorescent in situ hybridization

**References**

1. Regev A, Teichmann SA, Lander ES, Amit I, Benoist C, Birney E, Bodenmiller B, Campbell P, Carninci P, Clatworthy M, Clevers H, Deplancke B, Dunham I, Eberwine J, Eils R, Enard W, Farmer A, Fugger L, Göttgens B, Hacohen N, Haniffa M, Hemberg M, Kim S, Klenerman P, Kriegstein A, Lein E, Linnarsson S, Lundberg E, Lundberg J, Majumder P, Marioni JC, Merad M, Mhlanga M, Nawijn M, Netea M, Nolan G, Pe'er D, Phillipakis A, Ponting CP, Quake S, Reik W, Rozenblatt-Rosen O, Sanes J, Satija R, Schumacher TN, Shalek A, Shapiro E, Sharma P, Shin JW, Stegle O, Stratton M, Stubbington MJT, Theis FJ, Uhlen M, van Oudenaarden A, Wagner A, Watt F, Weissman J, Wold B, Xavier R, Yosef N. Human Cell Atlas Meeting Participants. 2017The Human Cell Atlas. *Elife*. :6.
2. Zeng H, Sanes JR. 2017Neuronal cell-type classification: challenges, opportunities and the path forward. *Nat Rev Neurosci*.
3. Macosko EZ, Basu A, Satija R, Nemesh J, Shekhar K, Goldman M, Tirosh I, Bialas AR, Kamitaki N, Martersteck EM, Trombetta JJ, Weitz DA, Sanes JR, Shalek AK, Regev A, McCarroll SA. 2015; Highly Parallel Genome-wide Expression Profiling of Individual Cells Using Nanoliter Droplets. *Cell*. 161:1202–1214. [PubMed: 26000488]
4. Trapnell C. 2015; Defining cell types and states with single-cell genomics. *Genome Res*. 25:1491–1498. [PubMed: 26430159]
5. Eberwine J, Sul J-Y, Bartfai T, Kim J. 2013; The promise of single-cell sequencing. *Nat Methods*. 11:25–27.
6. Marr C, Zhou JX, Huang S. 2016; Single-cell gene expression profiling and cell state dynamics: collecting data, correlating data points and connecting the dots. *Curr Opin Biotechnol*. 39:207–214. [PubMed: 27152696]
7. Marder E, Taylor AL. 2011; Multiple models to capture the variability in biological neurons and networks. *Nat Neurosci*. 14:133–138. [PubMed: 21270780]
8. Schulz DJ, Goaillard J-M, Marder E. 2006; Variable channel expression in identified single and electrically coupled neurons in different animals. *Nat Neurosci*. 9:356–362. [PubMed: 16444270]
9. Halpern KB, Shenhav R, Matcovitch-Natan O, Toth B, Lemze D, Golan M, Massasa EE, Baydatch S, Landen S, Moor AE, Brandis A, Giladi A, Avihail AS, David E, Amit I, Itzkovitz S. 2017; Single-cell spatial reconstruction reveals global division of labour in the mammalian liver. *Nature*. 542:352–356. [PubMed: 28166538]
10. Hardingham GE, Bading H. 2010; Synaptic versus extrasynaptic NMDA receptor signalling: implications for neurodegenerative disorders. *Nat Rev Neurosci*. 11:682–696. [PubMed: 20842175]
11. Rossey J, Pigeon SV, Davis DM, Gaus K. 2013; Super-resolution microscopy of the immunological synapse. *Curr Opin Immunol*. 25:307–312. [PubMed: 23746999]
12. Brownlie RJ, Zamojska R. 2013; T cell receptor signalling networks: branched, diversified and bounded. *Nat Rev Immunol*. 13:257–269. [PubMed: 23524462]
13. Lillemeier BF, Mörtelmaier MA, Forstner MB, Huppa JB, Groves JT, Davis MM. 2010; TCR and Lat are expressed on separate protein islands on T cell membranes and concatenate during activation. *Nat Immunol*. 11:90–96. [PubMed: 20010844]
14. Scott K, Zuker CS. 1998; Assembly of the Drosophila phototransduction cascade into a signalling complex shapes elementary responses. *Nature*. 395:805–808. [PubMed: 9796815]
15. Malbon CC. 2005; G proteins in development. *Nat Rev Mol Cell Biol*. 6:689–701. [PubMed: 16231420]
16. Collingridge GL, Isaac JTR, Wang YT. 2004; Receptor trafficking and synaptic plasticity. *Nat Rev Neurosci*. 5:952–962. [PubMed: 15550950]
17. Good MC, Zalatan JG, Lim WA. 2011; Scaffold proteins: hubs for controlling the flow of cellular information. *Science*. 332:680–686. [PubMed: 21551057]

18. Shah S, Lubeck E, Zhou W, Cai L. 2016; In Situ Transcription Profiling of Single Cells Reveals Spatial Organization of Cells in the Mouse Hippocampus. *Neuron*. 92:342–357. [PubMed: 27764670]
19. Moffitt JR, Hao J, Bambah-Mukku D, Lu T, Dulac C, Zhuang X. 2016; High-performance multiplexed fluorescence in situ hybridization in culture and tissue with matrix imprinting and clearing. *Proc Natl Acad Sci U S A*. 113:14456–14461. [PubMed: 27911841]
20. Lee JH, Daugharthy ER, Scheiman J, Kalhor R, Yang JL, Ferrante TC, Terry R, Jeanty SSF, Li C, Amamoto R, Peters DT, Turczyk BM, Marblestone AH, Inverso SA, Bernard A, Mali P, Rios X, Aach J, Church GM. 2014; Highly multiplexed subcellular RNA sequencing in situ. *Science*. 343:1360–1363. [PubMed: 24578530]
21. Ke R, Mignardi M, Pacureanu A, Svedlund J, Botling J, Wählby C, Nilsson M. 2013; In situ sequencing for RNA analysis in preserved tissue and cells. *Nat Methods*. 10:857–860. [PubMed: 23852452]
22. Milo, R, Phillips, R. *Cell Biology by the Numbers*. Garland Science, Taylor & Francis Group; 2016.
23. Chung K, Wallace J, Kim S-Y, Kalyanasundaram S, Andalman AS, Davidson TJ, Mirzabekov JJ, Zalocusky KA, Mattis J, Denisin AK, Pak S, Bernstein H, Ramakrishnan C, Grosenick L, Gradinaru V, Deisseroth K. 2013; Structural and molecular interrogation of intact biological systems. *Nature*. 497:332–337. [PubMed: 23575631]
24. Ertürk A, Becker K, Jährling N, Mauch CP, Hojer CD, Egen JG, Hellal F, Bradke F, Sheng M, Dödt H-U. 2012; Three-dimensional imaging of solvent-cleared organs using 3DISCO. *Nat Protoc*. 7:1983–1995. [PubMed: 23060243]
25. Renier N, Wu Z, Simon DJ, Yang J, Ariel P, Tessier-Lavigne M. 2014; iDISCO: a simple, rapid method to immunolabel large tissue samples for volume imaging. *Cell*. 159:896–910. [PubMed: 25417164]
26. Yang B, Treweek JB, Kulkarni RP, Deverman BE, Chen C-K, Lubeck E, Shah S, Cai L, Gradinaru V. 2014; Single-cell phenotyping within transparent intact tissue through whole-body clearing. *Cell*. 158:945–958. [PubMed: 25088144]
27. Murray E, Cho JH, Goodwin D, Ku T, Swaney J, Kim S-Y, Choi H, Park Y-G, Park J-Y, Hubbert A, McCue M, Vassallo S, Bakh N, Frosch MP, Wedeen VJ, Seung HS, Chung K. 2015; Simple, Scalable Proteomic Imaging for High-Dimensional Profiling of Intact Systems. *Cell*. 163:1500–1514. [PubMed: 26638076]
28. Hama H, Kurokawa H, Kawano H, Ando R, Shimogori T, Noda H, Fukami K, Sakaue-Sawano A, Miyawaki A. 2011; Scale: a chemical approach for fluorescence imaging and reconstruction of transparent mouse brain. *Nat Neurosci*. 14:1481–1488. [PubMed: 21878933]
29. Ke M-T, Fujimoto S, Imai T. 2013; SeeDB: a simple and morphology-preserving optical clearing agent for neuronal circuit reconstruction. *Nat Neurosci*. 16:1154–1161. [PubMed: 23792946]
30. Susaki EA, Tainaka K, Perrin D, Kishino F, Tawara T, Watanabe TM, Yokoyama C, Onoe H, Eguchi M, Yamaguchi S, Abe T, Kiyonari H, Shimizu Y, Miyawaki A, Yokota H, Ueda HR. 2014; Whole-brain imaging with single-cell resolution using chemical cocktails and computational analysis. *Cell*. 157:726–739. [PubMed: 24746791]
31. Murakami TC, Mano T, Saikawa S, Horiguchi SA, Shigeta D, Baba K, Sekiya H, Shimizu Y, Tanaka KF, Kiyonari H, Iino M, Mochizuki H, Tainaka K, Ueda HR. 2018; A three-dimensional single-cell-resolution whole-brain atlas using CUBIC-X expansion microscopy and tissue clearing. *Nat Neurosci*. 21:625–637. [PubMed: 29507408]
32. Crosetto N, Bienko M, van Oudenaarden A. 2015; Spatially resolved transcriptomics and beyond. *Nat Rev Genet*. 16:57–66. [PubMed: 25446315]
33. Chen F, Tillberg PW, Boyden ES. 2015; Optical imaging. Expansion microscopy. *Science*. 347:543–548. [PubMed: 25592419]
34. Hausen P, Dreyer C. 1981; The Use of Polyacrylamide as an Embedding Medium for Immunohistochemical Studies of Embryonic Tissues. *Stain Technol*. 56:287–293. [PubMed: 6171058]
35. Germroth PG, Gourdie RG, Thompson RP. 1995; Confocal microscopy of thick sections from acrylamide gel embedded embryos. *Microsc Res Tech*. 30:513–520. [PubMed: 7541260]



36. Tanaka T, Fillmore D, Sun S-T, Nishio I, Swislow G, Shah A. 1980; Phase Transitions in Ionic Gels. *Phys Rev Lett.* 45:1636–1639.
37. Ku T, Swaney J, Park J-Y, Albanese A, Murray E, Cho JH, Park Y-G, Mangena V, Chen J, Chung K. 2016; Multiplexed and scalable super-resolution imaging of three-dimensional protein localization in size-adjustable tissues. *Nat Biotechnol.* 34:973–981. [PubMed: 27454740]
38. Chang J-B, Chen F, Yoon Y-G, Jung EE, Babcock H, Kang JS, Asano S, Suk H-J, Pak N, Tillberg PW, Wassie AT, Cai D, Boyden ES. 2017; Iterative expansion microscopy. *Nat Methods.* 14:593–599. [PubMed: 28417997]
39. Cohen Y, Ramon O, Kopelman IJ, Mizrahi S. 1992; Characterization of inhomogeneous polyacrylamide hydrogels. *J Polym Sci B Polym Phys.* 30:1055–1067.
40. Tillberg PW, Chen F, Piatkevich KD, Zhao Y, Yu C-CJ, English BP, Gao L, Martorell A, Suk H-J, Yoshida F, DeGennaro EM, Roossien DH, Gong G, Seneviratne U, Tannenbaum SR, Desimone R, Cai D, Boyden ES. 2016; Protein-retention expansion microscopy of cells and tissues labeled using standard fluorescent proteins and antibodies. *Nat Biotechnol.* 34:987–992. [PubMed: 27376584]
41. Zhao Y, Bucur O, Irshad H, Chen F, Weins A, Stancu AL, Oh E-Y, DiStasio M, Torous V, Glass B, Stillman IE, Schnitt SJ, Beck AH, Boyden ES. 2017; Nanoscale imaging of clinical specimens using pathology-optimized expansion microscopy. *Nat Biotechnol.* 35:757–764. [PubMed: 28714966]
42. Chozinski TJ, Halpern AR, Okawa H, Kim H-J, Tremel GJ, Wong ROL, Vaughan JC. 2016; Expansion microscopy with conventional antibodies and fluorescent proteins. *Nat Methods.* 13:485–488. [PubMed: 27064647]
43. Freifeld L, Odstrcil I, Förster D, Ramirez A, Gagnon JA, Randlett O, Costa EK, Asano S, Celiker OT, Gao R, Martin-Alarcon DA, Reginato P, Dick C, Chen L, Schoppik D, Engert F, Baier H, Boyden ES. 2017; Expansion microscopy of zebrafish for neuroscience and developmental biology studies. *Proc Natl Acad Sci U S A.* 114:E10799–E10808. [PubMed: 29162696]
44. Deshpande T, Li T, Herde MK, Becker A, Vatter H, Schwarz MK, Henneberger C, Steinhäuser C, Bedner P. 2017; Subcellular reorganization and altered phosphorylation of the astrocytic gap junction protein connexin43 in human and experimental temporal lobe epilepsy. *Glia.* 65:1809–1820. [PubMed: 28795432]
45. Crittenden JR, Tillberg PW, Riad MH, Shima Y, Gerfen CR, Curry J, Housman DE, Nelson SB, Boyden ES, Graybiel AM. 2016; Striosome-dendron bouquets highlight a unique striatonigral circuit targeting dopamine-containing neurons. *Proc Natl Acad Sci U S A.* 113:11318–11323. [PubMed: 27647894]
46. Moses MJ, Counce SJ, Paulson DF. 1975; Synaptonemal complex complement of man in spreads of spermatocytes, with details of the sex chromosome pair. *Science.* 187:363–365. [PubMed: 1111110]
47. Cahoon CK, Yu Z, Wang Y, Guo F, Unruh JR, Slaughter BD, Hawley RS. 2017; Superresolution expansion microscopy reveals the three-dimensional organization of the *Drosophila* synaptonemal complex. *Proc Natl Acad Sci U S A.* 114:E6857–E6866. [PubMed: 28760978]
48. Tsanov N, Samacoits A, Chouaib R, Traboulsi A-M, Gostan T, Weber C, Zimmer C, Zibara K, Walter T, Peter M, Bertrand E, Mueller F. 2016; smiFISH and FISH-quant - a flexible single RNA detection approach with super-resolution capability. *Nucleic Acids Res.* 44:e165. [PubMed: 27599845]
49. Chen F, Wassie AT, Cote AJ, Sinha A, Alon S, Asano S, Daugharthy ER, Chang J-B, Marblestone A, Church GM, Raj A, Boyden ES. 2016; Nanoscale imaging of RNA with expansion microscopy. *Nat Methods.* 13:679–684. [PubMed: 27376770]
50. Wang G, Moffitt JR, Zhuang X. 2018; Multiplexed imaging of high-density libraries of RNAs with MERFISH and expansion microscopy. *Sci Rep.* 8:4847. [PubMed: 29555914]
51. Kosik KS. 2016; Life at Low Copy Number: How Dendrites Manage with So Few mRNAs. *Neuron.* 92:1168–1180. [PubMed: 28009273]
52. Buxbaum AR, Yoon YJ, Singer RH, Park HY. 2015; Single-molecule insights into mRNA dynamics in neurons. *Trends Cell Biol.* 25:468–475. [PubMed: 26052005]



53. Zhang YS, Chang J-B, Alvarez MM, Trujillo-de Santiago G, Aleman J, Batzaya B, Krishnadoss V, Ramanujam AA, Kazemzadeh-Narbat M, Chen F, Tillberg PW, Dokmeci MR, Boyden ES, Khademhosseini A. 2016; Hybrid Microscopy: Enabling Inexpensive High-Performance Imaging through Combined Physical and Optical Magnifications. *Sci Rep.* 6:22691. [PubMed: 26975883]
54. Halpern AR, Alas GCM, Chozinski TJ, Paredez AR, Vaughan JC. 2017; Hybrid Structured Illumination Expansion Microscopy Reveals Microbial Cytoskeleton Organization. *ACS Nano.* 11:12677–12686. [PubMed: 29165993]
55. Wang IE, Lapan SW, Scimone ML, Clandinin TR, Reddien PW. 2016; Hedgehog signaling regulates gene expression in planarian glia. *Elife.* :5.
56. Suofu Y, Li W, Jean-Alphonse FG, Jia J, Khattar NK, Li J, Baranov SV, Leronni D, Mihalik AC, He Y, Cecon E, Wehbi VL, Kim J, Heath BE, Baranova OV, Wang X, Gable MJ, Kretz ES, Di Benedetto G, Lezon TR, Ferrando LM, Larkin TM, Sullivan M, Yablonska S, Wang J, Minnigh MB, Guillaumet G, Suzenet F, Richardson RM, Poloyac SM, Stolz DB, Jockers R, Witt-Enderby PA, Carlisle DL, Vilardaga J-P, Friedlander RM. 2017; Dual role of mitochondria in producing melatonin and driving GPCR signaling to block cytochrome c release. *Proc Natl Acad Sci U S A.* 114:E7997–E8006. [PubMed: 28874589]
57. Decarreau J, Wagenbach M, Lynch E, Halpern AR, Vaughan JC, Kollman J, Wordeman L. 2017; Corrigendum: The tetrameric kinesin Kif25 suppresses pre-mitotic centrosome separation to establish proper spindle orientation. *Nat Cell Biol.* 19:740.
58. Kumar A, Kim JH, Ranjan P, Metcalfe MG, Cao W, Mishina M, Gangappa S, Guo Z, Boyden ES, Zaki S, York I, García-Sastre A, Shaw M, Sambhara S. 2017; Influenza virus exploits tunneling nanotubes for cell-to-cell spread. *Sci Rep.* 7:40360. [PubMed: 28059146]
59. Artur CG, Womack T, Zhao F, Eriksen JL, Mayerich D, Shih W-C. 2018; Plasmonic nanoparticle-based expansion microscopy with surface-enhanced Raman and dark-field spectroscopic imaging. *Biomed Opt Express.* 9:603. [PubMed: 29552397]
60. Sümbül U, Roussien D, Chen F, Barry N, Boyden ES, Cai D, Cunningham JP, Paninski L. 2016; Automated scalable segmentation of neurons from multispectral images. *Adv Neural Inf Process Syst.*
61. Unnersjö-Jess D, Scott L, Sevilla SZ, Patrakka J, Blom H, Brismar H. 2017; Confocal super-resolution imaging of the glomerular filtration barrier enabled by tissue expansion. *Kidney Int.*
62. Villaseñor R, Schilling M, Sundaresan J, Lutz Y, Collin L. 2017; Sorting Tubules Regulate Blood-Brain Barrier Transcytosis. *Cell Rep.* 21:3256–3270. [PubMed: 29241551]
63. Gao R, Asano SM, Boyden ES. 2017; Q&A: Expansion microscopy. *BMC Biol.* 15:50. [PubMed: 28629474]
64. ExpansionMicroscopy.org. Physical Specimen Expansion Enabling 3-D Large Volume, Nanoscale Imaging [Internet]. Available from: <http://expansionmicroscopy.org/>

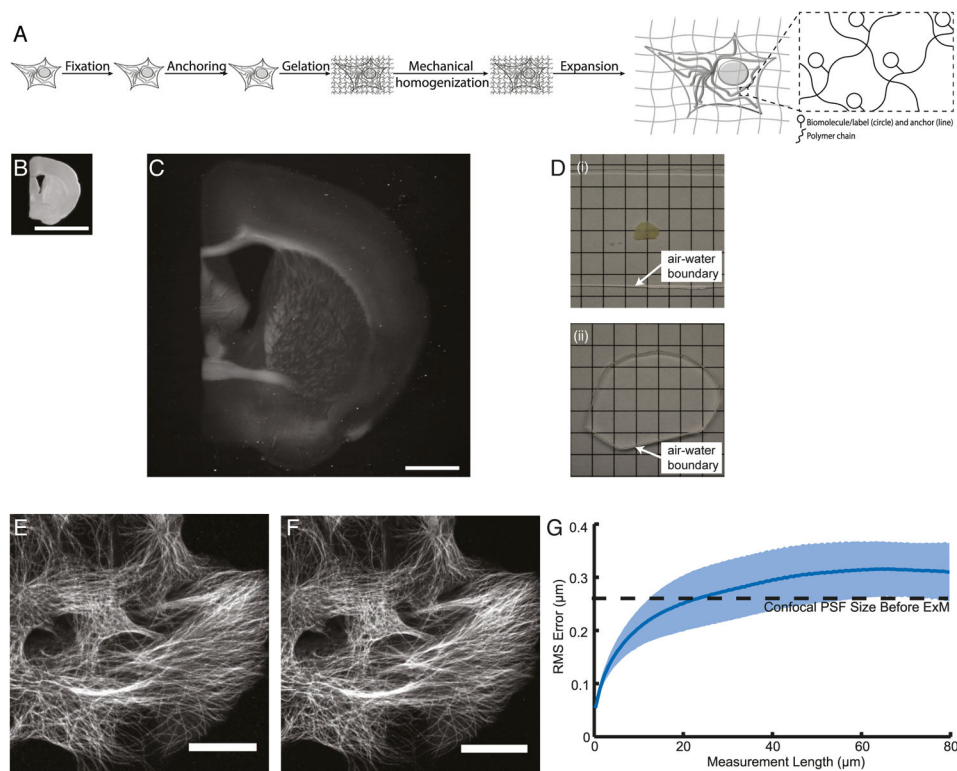


**Figure 1.**

Overview of expansion microscopy mechanism and process. (A) The biological specimen is chemically fixed, then treated with compounds to bind key biomolecules/labels of interest. A polyelectrolyte hydrogel is formed in situ, followed by proteolytic digestion and expansion in water. (B) Photograph of fixed mouse brain slice. (C) The specimen of B after expansion. (D) Expansion significantly reduces scattering of the sample, since the sample is mostly water. A 200  $\mu\text{m}$  fixed brain slice is opaque primarily due to scattering (i). However, the post-ExM sample is transparent (ii). (E, F) Confocal image of microtubules in cultured HEK293 cells before (E) and after (F) expansion. (G) RMS length measurement error of pre- versus post-ExM confocal images of cultured cells (blue line, mean; shaded area, standard deviation;  $n = 4$  samples). Scale bars: (B) and (C) 5 mm, in physical size units. (E) 20  $\mu\text{m}$ ; (F) 20  $\mu\text{m}$  in biological units (physical size post-expansion, 81.6  $\mu\text{m}$ ). Panel A adapted from ref. [63] and [40]. Panels B–G adapted from ref. [33].

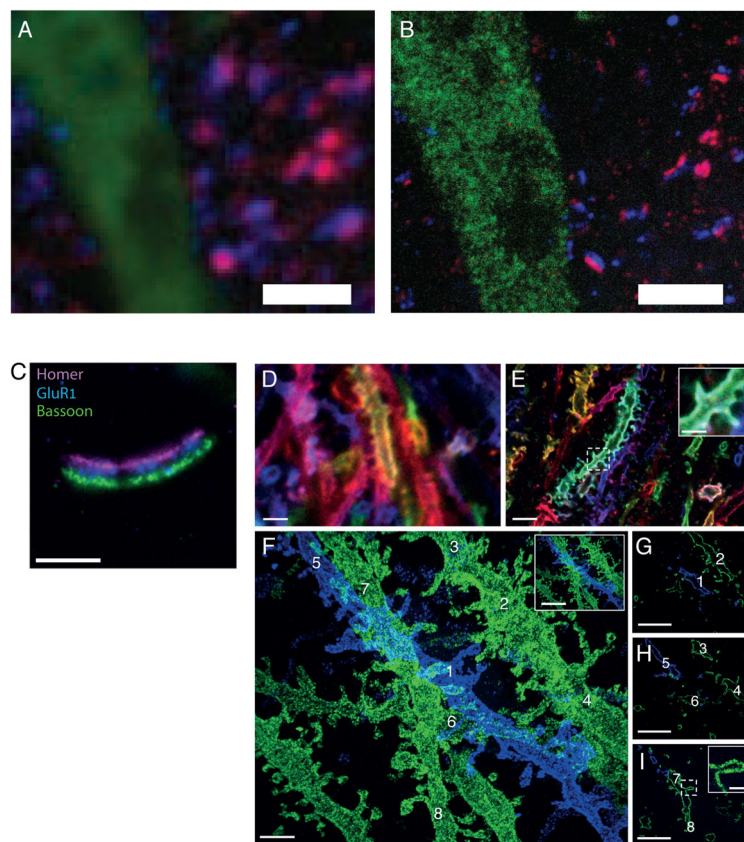


**Figure 2.**

Nanoscale detection of proteins with ExM and iterative ExM (iExM). Pre- (A) versus post- (B) expansion confocal fluorescence images of Thy1-YFP mouse brain slice, stained with presynaptic (anti-Bassoon, blue) and postsynaptic (anti-Homer1, red) markers, in addition to antibody to GFP (green). (C) Epifluorescence image of cultured hippocampal neurons stained with antibodies against Homer1 (magenta), glutamate receptor 1 (GluR1, blue), and Bassoon (green), after ~13-fold expansion via iExM. (D) Confocal image of immunostained Emx1-Cre mouse hippocampus with neurons expressing membrane-bound fluorescent proteins (Brainbow AAVs) before expansion. Blue, EYFP; red, TagBFP; green, mTFP. (E) As in D, but expanded 4.5-fold. Inset shows a magnified image of a spine in the dotted box of E. (F–I) Confocal z-stack image of 20-fold-expanded mouse hippocampal circuitry with labeled EYFP (blue) and mCherry (green). (F) Maximum intensity projection of the stack shown in (G–I). Inset in F shows a demagnified view of the image of F with the same scale bar as D and E. Inset of I shows a magnified view of a spine in the dotted box of I. Scale bars (A) 2.5  $\mu\text{m}$ ; (B) 2.5  $\mu\text{m}$  (physical size post-expansion 10.0 $\mu\text{m}$ ); (C) 1 $\mu\text{m}$ ; (D) and (E) 3 $\mu\text{m}$ , inset of E 1 $\mu\text{m}$ ; (F) 1 $\mu\text{m}$ , inset 3 $\mu\text{m}$ ; (G)–(I) 3 $\mu\text{m}$ , inset of I 0.5 $\mu\text{m}$ . Panels A–B adopted from ref. [33]; panels C–I adapted from ref. [38].

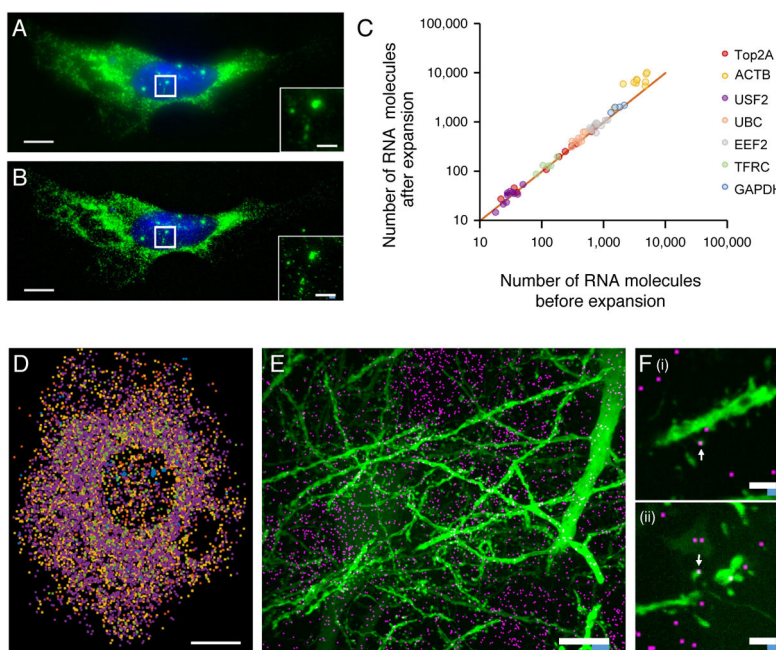


**Figure 3.**

Nanoscale and multiplexed detection of RNA with ExFISH. (A) smFISH image of ACTB before expansion of a cultured HeLa cell. Inset shows zoomed-in region, highlighting transcription sites in nucleus. (B) As in A, using ExFISH. (C) smFISH counts before versus after expansion for seven different transcripts ( $n = 59$  cells; each symbol represents one cell). (D) Composite image showing ExFISH with serially delivered probes against six RNA targets in a cultured HeLa cell; colors are as follows: NEAT1, blue; EEF2, orange; GAPDH, yellow; ACTB, purple; UBC, green; USF2, light blue. (E) Confocal image of hippocampal tissue showing colocalized Dlg4 puncta (magenta) overlaid on YFP (green) in Thy1-YFP mouse tissue. (F) Dendrites with Dlg4 mRNA localized to spines (arrows). (i), (ii), two representative examples. Scale bars: (A) and (B) 10  $\mu\text{m}$  (expansion factor, 3.3 $\times$ ), inset 2  $\mu\text{m}$ ; (D) (expanded coordinates) 20  $\mu\text{m}$ . (E) 10  $\mu\text{m}$  (expansion factor, 3 $\times$ ; white bar, biological scale; blue bar, physical scale); (F) 2  $\mu\text{m}$  (expansion factor, 3 $\times$ ). Adapted from ref. [49].



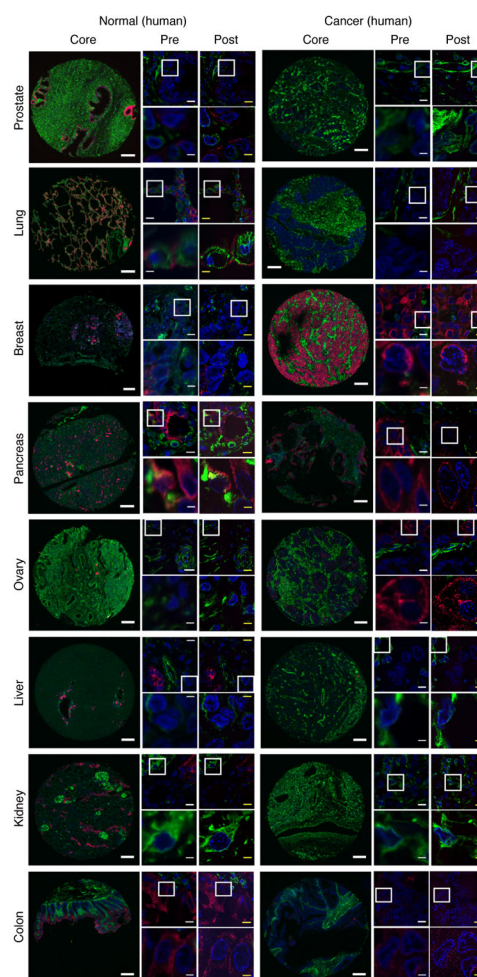


**Figure 4.**

Imaging of human tissue types using pathology-optimized expansion microscopy. Images of various tissue types for both normal (left images) and cancerous (right images) tissues from human patients. Within each block of images for a given tissue  $\times$  disease type, there are five images shown. The left-most of the five images shows a core from a tissue microarray (scale bar, 200  $\mu\text{m}$ ). The middle column within the five images shows two images, the top of which is a small field of view (scale bar, 10  $\mu\text{m}$ ), and the bottom of which zooms into the area outlined in the top image by a white box (scale bar, 2.5  $\mu\text{m}$ ). The right column within the five images shows the same fields of view as are shown in the middle column, but postexpansion (yellow scale bars: top images, 10–12.5  $\mu\text{m}$ ; bottom images, 2.5–3.1  $\mu\text{m}$ ). Physical size postexpansion: top images, 50  $\mu\text{m}$ ; bottom images, 12.5  $\mu\text{m}$ ; expansion factors 4.0–5.0 $\times$  (there is some sample-to-sample variability in expansion factor; in practice it is easy to measure the expansion factor for a given specimen: simply take a low-magnification image before you expand, and another low-magnification image after you expand, and compute the ratio of an easily seen feature, pre-expansion vs. post-expansion); Blue, DAPI; green, vimentin; magenta, KRT19. Adapted from ref. [41].